Mathematical Biosciences and Engineering

http://www.aimspress.com/journal/mbe

MBE, 20(2): 3638–3660.
DOI: 10.3934/mbe.2023170
Received: 12 October 2022
Revised: 01 November 2022
Accepted: 24 November 2022
Published: 09 December 2022

Research article

Teleoperation control of a wheeled mobile robot based on Brain-machine Interface

Su-na Zhao[1], Yingxue Cui[1], Yan He[1], Zhendong He[1], Zhihua Diao[1], Fang Peng[2,*] and Chao Cheng[3,4,*]

[1] College of Electrical and Information Engineering, Zhengzhou University of Light Industry, Zhengzhou 450000, China

[2] Zhongshan Institute, University of Electronic Science and Technology of China, Zhongshan 528402, China

[3] Key Laboratory of Bionic Engineering, Ministry of Education, Jilin University, Changchun 130022, China

[4] Weihai Institute for Bionics, Jilin University, Weihai 264402, China

* **Correspondence:** Email: fion_ peng@163.com, chengchao@jlu.edu.cn.

Abstract: This paper presents a novel teleoperation system using Electroencephalogram (EEG) to control the motion of a wheeled mobile robot (WMR). Different from the other traditional motion controlling method, the WMR is braked with the EEG classification results. Furthermore, the EEG will be induced by using the online BMI (Brain Machine Interface) system, and adopting the non-intrusion induced mode SSVEP (steady state visually evoked potentials). Then, user's motion intention can be recognized by canonical correlation analysis (CCA) classifier, which will be converted into motion commands of the WMR. Finally, the teleoperation technique is utilized to manage the information of the movement scene and adjust the control instructions based on the real-time information. Bezier curve is used to parameterize the path planning of the robot, and the trajectory can be adjusted in real time by EEG recognition results. A motion controller based on error model is proposed to track the planned trajectory by using velocity feedback control, providing excellent track tracking performance. Finally, the feasibility and performance of the proposed teleoperation brain-controlled WMR system are verified using demonstration experiments.

Keywords: BMI; SSVEP-based system; Bezier curve; CCA

1. Introduction

Technology for brain-controlled external devices has received a lot of attention because it allows people with neurological and movement disorders to interact with their surroundings and control devices with their thoughts. Mechanical control systems are used as the natural and conventional control methods for the average population to communicate between the terminal device and environment.

Brain-controlled technology, which can provide a directly mean of communication between brain and external environment for the people with movement disorders and neurological diseases, such as robot manipulation [1], robot navigation [2–5], wheelchair [6–8], speller [9], lower limb exoskeleton [10]. The EEG was used by the brain-actuated system to encode the user's intended movement, which could then be translated into commands to control the terminal device from moving. In [1], by using SSVEP protocol, a noninvasive brain-actuated system is designed to control the robot manipulation with two-arm to perform the bimanual relative manipulation tasks. The authors make the research on the problem of mobile robot navigation based on BMI. In [2], a BMI control strategy is proposed to control mobile robot to realize automatic navigation and positioning in urban corridor environment by using SSVEP protocol. In [3], an asynchronous direct-control navigation system for humanoid robot based EEG is applied to control the robot reached the goal in the indoor maze. In [4], authors proposed a new control strategy to lower the false positive rate, which can improve navigation performance, by taking into account the nature of BMI output. In [5], the EEG based online BMI system was applied on the leader-follower robots to complete cooperative motion control with demand that the two robots remain 2 meters relative to each other. Intelligent wheelchair based on EEG controlling is one of the classic applications of brain control technology. In [6], by using Bayesian method, a shared controller is proposed that employs a hierarchical brain control mechanism with feedback rules to obtain precise control commands. In [7], a shared control method combined with polynomials trajectory planning algorithm is used to realize the motion of brain-controlled wheelchair. Authors of [8], design and build the EEG actuated wheelchair, which can actuate the wheelchair to navigate by EEG in indoor office or hospital environment.

Brain-controlled technology is now being used in the fields of prosthetic devices and rehabilitation. Researchers have developed the brain-controlled spelling system and brain-controlled prosthesis system to assist the communication functions of patients with severe motor disorders. In [9], a dynamically SSVEP brain-controlled system with the new signal processing method CCA-RV is proposed to enhance the speed and accuracy of the speller. In [10], the rhesus macaques controlled the lower limb exoskeketon under both brain control and automated actuation by staring the curse on the screen.

In brain-actuated system, the basic but important step is EEG recognition, which can decode and convert the motor intention into control commands that can drive external devices (for instance, wheelchair, type, manipulator). Brain computer interfaces can be classified as either spontaneous or induced depending on how the EEG signal is produced. SSVEP is one of the classical signals of induced pattern, and is widely utilized in brain-controlled system for frequency tagging research, because it can transfer information with high accuracy. In this paper, simulate the control of WMR direction in the process of human driving, four flickering rectangular display blocks which located on the display are used for evoking EEG signal.

In SSVEP brain-controlled system, users are concentrated on the visually evoked interface, so the teleoperation is utilized to expand the motion range of the brain-controlled mobile. In [11], the tele-

operation system can enable mobile robot obstacle avoidance by using a shared impedance control scheme. In [12], authors proposed a brain-driven teleoperation system, which enables the users control robots to operate remotely in the remote task space through the BMI. In general, the key technology of teleoperation involves image or video transmission and processing, which determine the performance of the visual servoing. In [13, 14], the navigation and monitoring of a teleoperation robot are made possible by using visual servoing feedback techniques. In [13], users face a screen that displays virtual environment in real time to induce EEG signals to control the wheelchair's movements. In [14], by using the remote display real-time 3D mobile platform models and continuous predictive display delay compensation to achieve the remote control of the robot.

Trajectory planning and trajectory tracking are also the key technologies for motion control of robot. Pure geometric trajectory planning, such as straight lines [15], cubic splines [16], polynomials [17], Bezier curb [18], which have been used to produce a continuously smooth trajectory. In reality, robot motion control is achieved by combining pure geometric trajectory planning with intelligent algorithms and controllers [15]. For example, polynomial parametrization and genetic algorithm are combined to propose a parallel parking trajectory planning algorithm for car-like robots. In [16], a nonholonomic path planning method based on cubic spirals and line segments is proposed for car-like mobile robot. In [17], polynomial interpolation function fused with the traditional cuckoo search algorithm to optimize the trajectory of a robot. Bezier, a classical mathematical curve, is often used in computer graphics, robotics for animation and trajectory planning [18]. The intelligence of a brain-controlled robot can be increased if the EEG signal classification results and trajectory planning can be combined.

This paper proposes the control framework for teleoperation based on brain-machine interfacing. The visual feedback loop produces the environment information of motion space to the user, which enables the operator to know the environmental information of the movement space and adjust the brain induced mode to produce different control signals. The online BMI connecting and analyzing the EEG data to decode the human intentions which are convert to motion commands for the teleoperated robot under the SSEVP model. Bezier curve can parameterize the motion command and the motion controller to realize reference trajectory tracking. A mechanism that imitate the driving behavior of human is adopt, the brain is like the steering wheel, the camera is like the eye, then the motion command is generated in real time through the EEG signal to control the robot's movement in the motion space. Five subjects were used in extensive experimental studies to gauge the effectiveness of the suggested system.

In summary of the above mentioned literature, most of the research on brain-controlled external devices is divided into two parts: BCI and motion control of external devices. In this paper, the classification results of EEG signals are parameterized to plan trajectories. This combines the brain-computer interface with the motor control of external devices. It simulates human driving mechanism and provides a kind of brain motion control mode for brain controlled robot navigation system. The main contributions of this paper are summarized in the revision as:
(I) a parametric trajectory planning method based on the EEG signal recognition results is proposed, which combines the EEG classification results with Geometry curve;
(II) a motion control mechanism that simulates human driving behavior is adopt, which uses the brain as the steering wheel to improve the intelligence of brain control system.

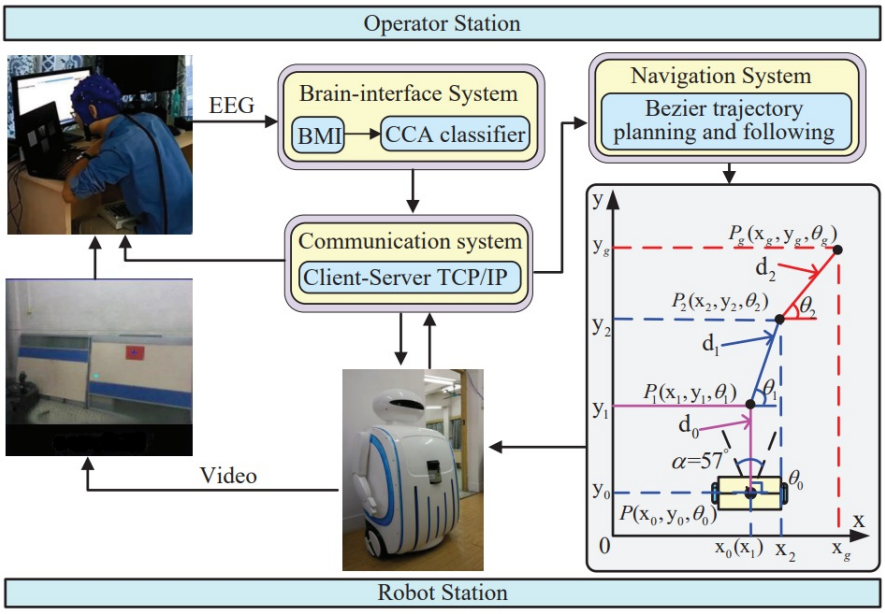

Figure 1. The Brain-actuated system of mobile robot.

2. Structure of Brain-actuated robot system

A closed-loop brain-controlled robot system is represented by the overall control structure in Figure 1. Mobile robot and BMI make up the bulk of the Brain-actuated system.

For the BMI, the device with 40 channels electrode cap and NuAmps device (Compumedics, Neuroscan Inc., Australia) is used to collect EEG. The electrodes' impedance of the cap is set below 5 $k\Omega$, Cz is defined as the reference signal passage, and with the sampling frequency is 500 Hz. The visual functional area is primarily distributed in the occipital lobe, and the visual center is a group of visual-related nerve cells in the cerebral cortex. So, datas of the four electrodes Pz, O1, O2, and Oz, were identified as the motion commands, because these four electrodes are located in the occipital lobe of the human brain. A bandpass filter (5 Hz to 30 Hz) and a notch filter of 50 Hz, are utilized to eliminate noise and improve signal-to-noise ratio. The CCA classification algorithm can identify the movement intention present in the EEG. The recognition results are converted to motion commands to drive the robot to the target point. The visual feedback technology is used to realize the real-time monitoring of robot motion space. The Kinect can transfer images and provide the live video on the center of the screen to operator as visual feedback. Users can track the movement scene information in real time by focusing on the screen.

3. Brain Machine Interface

The main function of the BMI is including: collecting EEG signals, preprocessing, classification, and conversion of recognition results to motion control commands [19].

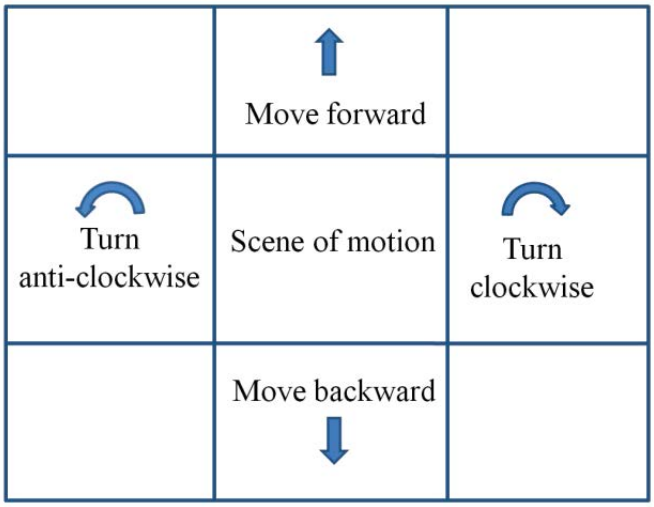

Figure 2. The visual-interface of BMI.

3.1. Graphical interface and teleoperation

The SSVEP mode of evoked EEG signal generation links the frequency of the stimulus to the continuous neuronal activity of the visual cortex. When the person's visual attention is focused on visual stimulus that given at a fixed frequency, the brain will generate the signals related to the fundamental frequency or multiple frequency of the stimulus frequency. The display screen, which includes stimulus frequency and visual feedback, is depicted in Figure 2. During the SSVEP process, users only need to focus on the different visual stimulation module with specific frequencies, then the operators' brain can generate continuous EEG related to stimulus frequency.

In Figure 2, four stimulus modules (four rectangles) with size 10 $cm \times 8$ cm and fixed frequency are distributed around the display to induce electrical signals in the brain. Limited by the refresh rate of the display, the four stimulus frequencies are determined according to the formula:

$$F_{sti} = \frac{60}{n} \tag{3.1}$$

where F_{sti} denotes the stimulus frequencies, and n is positive integer. In this paper, the parameter n = 4, 5, 6, 7, so the corresponding stimulus frequencies are 8.57 Hz, 10 Hz, 12 Hz, 15 Hz, respectively.

The video feedback of motion scenes in real-time is displayed in the rectangle in the center of the screen and is used to enable teleoperation. In BIM controlled robot system, the teleoperation technique is utilized to know the scene of the motion space, such as the position of the target point and distribution of obstacles. In this paper, a visual feedback-based BMI teleoperation system is designed and implemented. The visual perception sensor can feed back the environmental information to the operator, so as to adjust the stimulus module to change the robot motion control instructions, and realize the movement of the mobile robot is controlled by EEG.

3.2. EEG acquisition and recognition

To gather and process the raw EEG signal, a digital EEG recording device with 32 electrodes is evenly positioned on the user's scalp. The BMI system based on SSVEP model is used to detect EEG signals in the visual area of the occipital lobe to determine brain activity. The occipital region is the visual center of the brain, so EEG collected from four main electrodes (Pz, O1, O2, Oz) are used as the input signals for the CCA classifier.

The brain's neurons produce weak raw data, so an amplifier is required to amplify the original signal. In addition to amplification, an appropriately spatial filter is used to improve the signal-to-noise ratio (SNR). It's possible that EEG noise is a common occurrence, and the presence of artifacts results in low SNR. There are many spatial filtering methods for EEG signal, the Laplacian methods and common average reference (CAR) are the two most available methods [20]. In this study, the SNR and BMI performance are both improved by using the CAR. The CAR function is defined as follows:

$$V_i^{CAR} = V_i^{ER} - \frac{1}{n}\sum_{j=1}^{n} V_j^{ER} \tag{3.2}$$

here, n is the number of electrodes placed in the occipital region, V_i^{ER} is the potential of ith channel. In CAR, the average value of all electrodes is calculated and the noise is eliminated by removing the average value of all electrodes. Experimental results demonstrate that CAR outperforms all benchmark techniques and achieves the highest levels of classification accuracy.

3.3. CCA classification

CCA is a multivariate statistical analysis method that studies the correlation between two groups of variables and is also a dimensionality reduction technique. The essence of CCA is to select several representative comprehensive indicators (linear combination of variables) from two groups of random variables, and use the correlation between these indicators to express the correlation between the original two groups of variables. In this study, the collected signals are divided into four categories by calculating the correlation between the EEG data and the reference signals.

The collected EEG form a matrix X with $N \times M$, where N is the EEG channels and M is the number of the EEG samples in one group. First, define the following parameter variables: the stimulus frequency $f_i, i = 1, 2, \ldots, N_f$, the reference signals are $Y_i \subset R^{2N_h \times M}$ that N_h is the number of the sine harmonics and cosine harmonics components. In terms of defined variables, the reference reference signal is constructed as:

$$Y_{fi(t)} = \begin{bmatrix} \sin(2\pi \cdot f_i \cdot t) \\ \cos(2\pi \cdot f_i \cdot t) \\ \vdots \\ \sin(2\pi \cdot N_h \cdot f_i \cdot t) \\ \cos(2\pi \cdot N_h \cdot f_i \cdot t) \end{bmatrix}$$

among them, F_s is the sampling rate, t is the sampling time, $t = \frac{1}{F_s}, \frac{2}{F_s}, \cdots \frac{M}{F_s}$, $2N_h$ is the harmonics components.

For the two multidimensional variables X and $Y_{fi(t)}$, x, y are the linear combination of them.

$$x = X^T W_X \tag{3.3}$$

$$y = Y^T W_Y \tag{3.4}$$

The core of CCA algorithm is to find weight vector W_X and W_Y, so as to maximize the correlation $\rho(x, y)$ between x and y.

$$\max_{W_X, W_Y} \rho(x, y) = \frac{E[W^T X Y^T W_Y]}{\sqrt{E}[W_X^T X X^T W_X] E[W_Y^T Y Y^T W_Y]} \tag{3.5}$$

CCA is used to determine the canonical correlations between multichannel EEG and reference signals for each stimulus frequency of the SSVEP BMI. The frequency corresponding to the reference signal with the greatest correlation is the frequency of the EEG signal.

4. Motion planning

Motion planning includes trajectory planning and trajectory tracking, which decomposes the desired motion task into discrete motions that satisfy the motion constraints and may optimize one aspect of the motion. By inserting a number of points between the beginning and end points, trajectory planning generates instruction trajectories. Trajectory tracking the robot can track the planned trajectory accurately and in real time by selecting appropriate control algorithm and parameters.

4.1. Bezier trajectory planning

Based on mathematics, the Bezier curve can create complex smooth curves with just three points: the beginning, control, and goal [21, 22]. The curve passes through the beginning point and the end point, and is tangent to the two sides of the feature polygon. The control points determine the shape of the curve, changing the coordinates of a control point, the shape of the curve will change (points have overall control over the curve). This continuous high-order differentiability of Bezier can ensure the curve's radius varies smoothly and clearly, and the shape and order of the curve can be easily changed. Bezier have been widely used in path planning of mobile robots in recent years based on the geometric characteristics of the curves.

The parametric Bezier curve is expressed as:

$$P(u) = \sum_{i=0}^{n} J_i^n(u) B_i, 0 \le u \le 1 \tag{4.1}$$

u is the location parameter, i is the summation index, $J_i^n(u)$ is the i_{th} Bernstein function, B_i is the control points of the Bezier polygon.

Supposing there are $(n + 1)$ control points, nth Bezier is given as following:

$$J_i^n(u) = C_n^i u^i (1 - u)^{n-i} \tag{4.2}$$

$$C_n^i = \frac{n!}{i!\,(n - i)!} \tag{4.3}$$

here $u^i(1 - u)^{n-i}$ denotes the blending function, and the C_n^i is the coefficient.

When planning the path of the robot, the geometric properties of the curve are used. The curve starts at the first control point and ends at the last control point. The first and last edges of the feature

polygon are, respectively, on the tangents of the curves at the starting and ending points. Given two points, P_0 and P_1, the 1_{th} Bezier is a straight line that goes through these two points. The equation is:

$$B(u) = P_0 + (P_1 - P_0)u = (1 - u)P_0 + tP_1 \tag{4.4}$$

Combined with the actual application of brain control system, we defined two parameters d and θ for the planned Bezier curve to simplify and parameterize the implementation of brain-actuated control. But also to mimic the walk of the human walking. Where d and θ are the distance and angle for one motion command.

$P_0(x_0, y_0, \theta_0)$ is the starting point, $P_1(x_1, y_1)$ is the goal point that can be calculated according to the following formula:

$$x_1 = d_0 \cos(\theta_0) \tag{4.5}$$

$$y_1 = d_0 \sin(\theta_0) \tag{4.6}$$

Then, the Bezier curve can be planned from (4.4). In order to parameterize trajectories, parameters d and θ are combined with the classification results of EEG.

4.2. Control strategy

The control strategy mimics the paradigm of the brain controlling a person's walking in order to show the intelligence of the brain-controlled robot. In the process of human movement, vision provides environmental information and plans the route, while the brain issues movement instructions to control body movement. In BMI system, the Kinect camera monitors environmental information and feeds it back to the brain to plan movement paths. The function of the brain in BMI is just like a sheering wheel, and its rotation depends on the change of the environment For example, when there is an obstacle, the steering wheel needs to be turned to adjust the direction of movement. The classification results are parameterized and combined with the parameters of the trajectory planning algorithm, and the controller which satisfied the nonholonomic constraint and kinematic can controlled the robot movement followed the planned trajectory.

The motion control of robot adopts the method of combining global trajectory planning with local trajectory planning. A global trajectory to the goal point will initially be generated when the goal is given. The robot's local trajectory is produced by the EEG recognition results which depend on the scene feedback of the robot's motion space, such as whether there are obstacles.

A parameterized Bezier curve of the EEG is planned as the motion trajectory from the starting point to the goal points. The mobile robot follows this trajectory based on brain-actuated. The trajectory should be smooth rather than zigzag in order to guarantee the effective performance of motion controlling. In actual application scenarios, users need to stare at the screen to elicit EEG signal to produce motion command, all the planned points can not be outside the visual view of the Kinect.

S is the initial point, G is the end point, it can plan a trajectory based Bezier which can be adjust timely by varying length d and angle θ. Defining two new variables, $\alpha(\kappa)$ and $\beta(\kappa)$:

$$\alpha(\kappa) \in [1, -1] \tag{4.7}$$

$$\beta(\kappa) \in [1, -1] \tag{4.8}$$

$\alpha(\kappa)$ and $\beta(\kappa)$ will effect the shape of the curve. $\alpha(\kappa) \in [1, -1]$ is mainly controls the distance change of the trajectory, that is robot moves forward or backward. When $\alpha(\kappa) = 1$, the length increases, $\alpha(\kappa) = -1$, the length decreases. $\beta(\kappa) \in [1, -1]$ is mainly controlled the angle change of the trajectory, that is robot turns left or right. When $\beta(\kappa) = 1$, the angle increases, $\alpha(\kappa) = -1$, the length decreases. The "1" or "-1" depends on the classification result of BMI. In this way, the classification results of EEG signals can be used to parameterize the trajectory of the robot.

In process of trajectory planning, $\theta(k)$ and $d(k)$ in time k will determine the Bezier polygon's orientation in time $k + 1$:

$$\theta(\kappa + 1) = \alpha(\kappa)\Delta(\theta) \tag{4.9}$$

$$d(\kappa + 1) = \beta(\kappa)\Delta(d) \tag{4.10}$$

where, $\Delta(\theta)$ is a preset change in angle rotation angle which related to the EEG classification results. Therefore, the values of $\theta(k + 1) = \pi/2$, $\theta(k + 1) > \pi/2$, $\theta(k + 1) < \pi/2$ respectively represent the three motion states of the robot: go forward, turn left and turn right with certain speed along the planned trajectory.

Robot moves along the planned trajectory in processing of trajectory tracking. At the same time, visual feedback provides the information of the movement environment. Based on the information, operators can know the goal point and the actual situation of the motion scene, so as to determine to stare the stimulus module in the visual interface to generate different control commands, which will change the planned trajectory.

For example, in time k, the robot moves along the trajectory in point P_i. Defining Δt is the instant, the Δs and v are the corresponding distance and average velocity in Δt. In the next infinitesimal time, the robot would reach the next point P_{i+1}, then the infinitesimal displacement Δs over that time is expressed as:

$$\Delta s = \upsilon\Delta(t) \tag{4.11}$$

Then, for the robot, the angular orientation on the trajectory can be calculated by the slope at that point. Defining $d\theta$ is the variation rate in angular, ω is the angular velocity of the robot is expressed as:

$$\omega = \frac{d\theta}{dt} \tag{4.12}$$

5. Control development

A controlled process is made up of moving robots and their surroundings. The core task of BMI system is controlling the robot move to the target point according to the trajectory planned by the EEG.

5.1. Kinematic model of robot

In this paper, the mobile robot system consists of mechanical system, sensing system and control system. The mobile robot has two wheels which are adopt the differential drive model with kinematics and driven by motors independently to realize the coordination of motion and body.

To analyze the kinematic model of a wheeled mobile robot, the coordinated cartesian system and robot body are both established in motion space. For the robot body coordinate system, the reference

center is located in the middle of the axis of the two driving wheels. The robot's configuration is defined as:

$$P = [x_p, y_p, \theta_p]^T \tag{5.1}$$

Typically, it is assumed that the body of the two-wheeled robot has no slippage. Under that assumption and specified coordinate system, in the point P, the orientation angle θ_p with respect to the x axis. The robot's kinematic model can be described as follow:

$$\begin{aligned} \dot{x_p} &= \upsilon_p \cos(\theta_p) \\ \dot{y_p} &= \upsilon_p \sin(\theta_p) \\ \dot{\theta_p} &= \omega_p \end{aligned} \tag{5.2}$$

The linear velocity and angular velocity in the point P are υ_p and ω_p. Eliminating υ_p in Eq (5.2), the Eq (5.2) is simplified and the nonholonomic constraints on the robot can be computed as follows:

$$\dot{x_p} \sin(\theta_p) - \dot{y_p} \cos(\theta_p) = 0 \tag{5.3}$$

Then, the kinect model of the robot in Eq (5.2) can be described as follows.

$$\dot{P} = \begin{bmatrix} \cos\theta_p \\ \sin\theta_p \\ 0 \end{bmatrix} \upsilon + \begin{bmatrix} 0 \\ 0 \\ 1 \end{bmatrix} \omega \tag{5.4}$$

5.2. Control method based on Lyapunov

The inverse design method is used to decompose the kinematics model [23], and the speed tracking controller is designed to track the planned trajectory. The reference pose is obtained by calculating the planned trajectory, and the actual pose is obtained by sensors which are equipped on the robot. The objective function is considered to be the transfer equation of pose error, which can be obtained.

Based on the planned trajectory, in point P, the desired pose of the robot is:

$$P_d = (x_d, y_d, \theta_d)^T \tag{5.5}$$

The core task of tracking is to control the speed error to zero. The input vector of the controller is $u_d = (\omega_d, v_d)^T$. Defining $P_e = [x_e, y_e, \theta_e]^T$ is the error between the reference and virtual states in point P, then the error will be written as:

$$\begin{bmatrix} x_e \\ y_e \\ \theta_e \end{bmatrix} = \begin{bmatrix} \cos\theta_p & \sin\theta_p & 0 \\ -\sin\theta_p & \cos\theta_p & 0 \\ 0 & 0 & 1 \end{bmatrix} \begin{bmatrix} x_d - x_p \\ y_d - y_p \\ \theta_d - \theta_p \end{bmatrix} \tag{5.6}$$

The kinematic error of the robot can be described as:

$$\begin{cases} \dot{x}_e = v_d \cos\theta_e - v_d + y_e \omega_d \\ \dot{y}_e = v_d \sin\theta_e - x_e \omega_d \\ \dot{\theta}_e = \omega_d - \omega_p \end{cases} \tag{5.7}$$

According to the inversion design method, the control law of the trajectory tracking controller is designed as:

$$\begin{bmatrix} \nu_c \\ \omega_c \end{bmatrix} = \begin{bmatrix} v_d \cos\theta_e + k_1 x_e \\ \omega_d + k_2 v_d y_e + k_3 \sin\theta_e \end{bmatrix}, \tag{5.8}$$

among them, k_1, k_2, k_3 are positive constants.

The controller for the differential mobile robot should be nonlinear, and the structure will depend on the chosen function [24]. The following candidate function is selected as follow:

$$V = \frac{k_2}{2}(x_e^2 + y_e^2) + (1 - \cos\theta_e) \tag{5.9}$$

It is obviously to see from Eq (5.9) that $V \geq 0$. At point P, if $P_e = 0$ then $V = 0$, and if $P_e \neq 0$ then $V > 0$. To calculate the derivative or differential of the Eq (5.9), and plug the trajectory tracking error into the equation [25, 26]. The differential equation is as following:

$$\dot{V} = -k_1 k_2 x_e^2 - k_3 sin\theta_e{}^2 \tag{5.10}$$

The Eq (5.10) can make the robot system asymptotic equilibrium point $P_e = 0$, that is control system error approximately to zero [27]. The proposed controller satisfies the nonholonomic constraint and kinematic of the mobile robot [28]. The non-negative property of Eq (5.9) ensures the stability of the motion system. Eqs (5.7) and (5.8) can prove the time derivative of above Lyapunov function is negative definite, i.e., $\dot{V} = -k_1 k_2 x_e^2 - k_3 \sin^2\theta_e \leq 0$. In this paper, after simulation and experimental debugging, parameters of motion controller are chosen as $k_1 = 1$, $k_2 = 2$, $k_3 = 3$.

6. Experiments verification

The effectiveness of the proposed barin-controlled robot system is tested through experiments. The brain-controlled robot system consists of three parts: EEG decoding, target point detection and motion control. Motor intention recognition based on EEG is the fundamental part, and the CCA method is used to classify EEG signals [29–31]. The Kinect camera monitors the motion scene in real time and transmits the video to the center of the stimuli interface. The given task is to teleoperate brake the robot to reach the given goal position by the subject's EEG. The results of the experiments demonstrated that a robot in motion space can be driven by the EEG.

6.1. Experimental setup

The experimental platform includes two parts: BMI and robot. The robot and hardware structure of system is shown in Figure 3. The BMI includes laptop and PC, laptop is used to provide a stimulus interface, and PC us used to generate and process of EEG. The robot control system uses BIS-6553 IPC (industrial computer) which produced by North China Industrial Control Company. The IPC is configured as follows: CPU is Intel core i7 processor, main frequency is 3.3 GHz, and it has 4 GB memory and 2 GB independent graphics card.

The mobile robot has two training wheels for balance as well as two driving wheels powered by servomotors. The driving wheels with a radius of 19.5 *cm* are installed on both sides of the robot chassis, and driven by 48 *V* rated voltage motors with a rated torque 72.1 *mNm/A* at 5200 *rpm*. Two counting incremental encoders are mounted on the motor shaft to calculate the position of the robots, and reduction ratio of motor is 85.55.

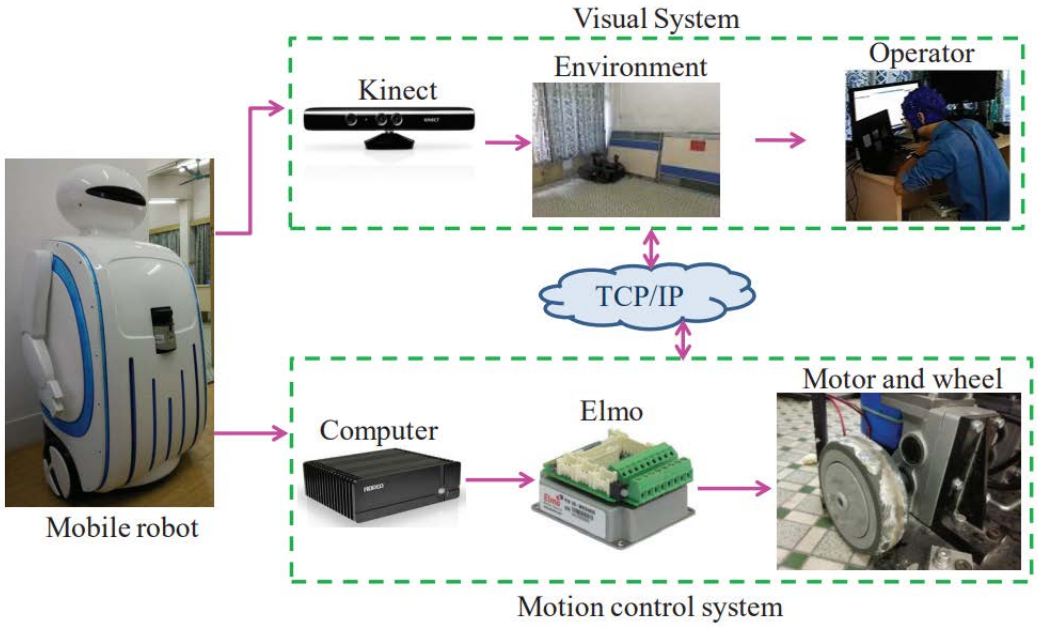

Figure 3. The robot and hardware structure of system.

6.2. EEG acquisition and analysis

Four stimulus modules are distributed over the display in Figure 2, which will induce signals with four stimulus frequencies. The subject decides which stimulus module to stare at and generates the corresponding command to control the motion of the mobile robot, according to the position of the target and the actual situation of the movement space. In the experiment, the subjects wear electrode caps to stare at the stimulate module, and the actual scene in the moving space is displayed in the middle area of the display by camera feedback. The Kinect visual sensor can transmit visual information of the motion environment in real-time.

Five subjects (1 female and 4 males in age range of 22–24) participated in the confirmatory experiment. The subjects were sitting on a comfortable chair under the condition of being relaxed and motionless, then staring at the stimulated indicators. By fixating eyes on the flashing stimulus, the subjects EEG signals corresponding to the stimulus frequencies will be induced. The collected EEG signals are shown in Figure 4.

One of the characteristics of the signals generated by SSVEP induced mode is that, even people who are not family with the electrical system, high classification results can be obtained without a long time of training and testing. Generally, subjects become familiar with the characteristics of the BMI system after a round of offline measurement. But, for the reason to ensure the performance of the brain control system, each subject collected 5 rounds of data in offline test. After the recognition rate of the offline test reached the requirement, subjects began to complete the brain-controlled teleoperation task, that is autonomously navigating the brain-controlled teleoperation mobile robot from the start to the goal point.

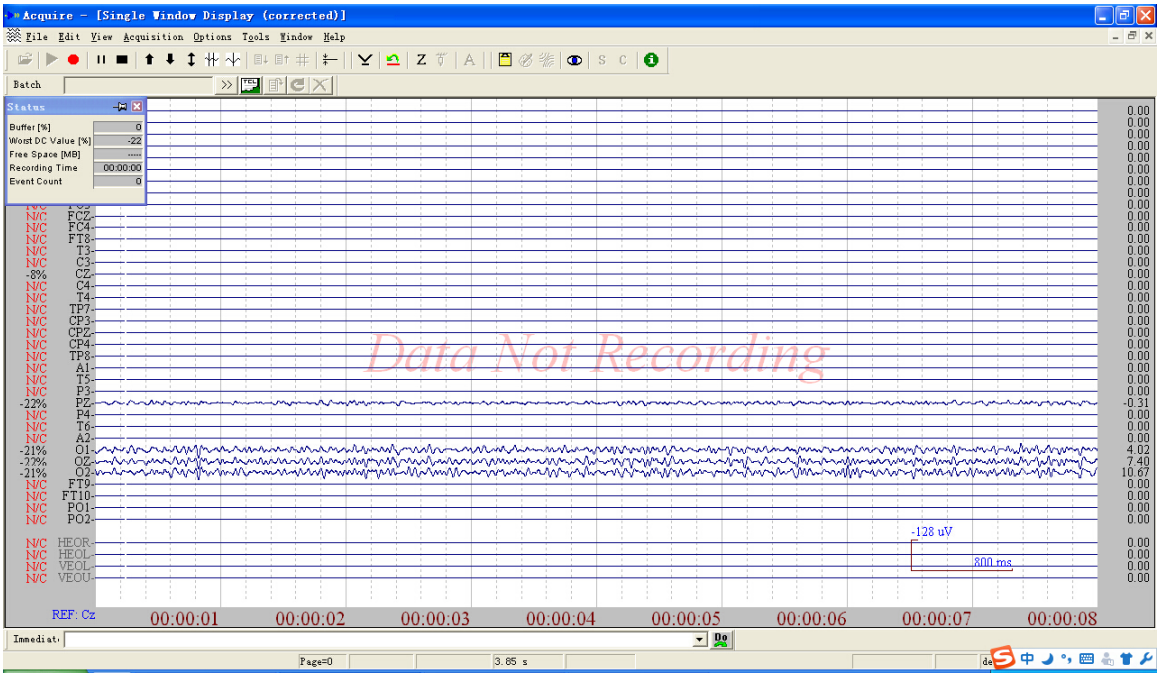

Figure 4. The collected EEG signals.

First, the subjects had to take an EEG offline test, and the experiment could be conducted normally only when the offline EEG recognition rate is more than 85%. BMI Noise in EEG may be a common activity, and the presence of artifacts lead to low SNR. It will directly affect the performance of robot motion system. Here, a new variable *ERA* (*EEGrecognitionaccuracy*) is defined to evaluate the performance of the classification algorithm, which can be expressed as following:

$$ERA = \frac{TR}{RR} \times 100\% \tag{6.1}$$

RR and *TR* represent all the classification results and correct classification results of the collected EEG respectively. The signal sampling rate is 512 Hz, and per period 800 data samples were analysed and identified. Therefore, it is simple to calculate that it will take 1.56 s to produce a robot motion command.

Figure 5 displays the overall average recognition accuracy for all subjects. From Figure 5, it is shown that the average recognition accuracy of all the user's is more than 85%. In contrast, the ERA of subjects 1 and 2 are higher than the other 3 subjects. This is because subjects 1 and 2 are have taken part in such experiment many times. For SSVEP, users do not need special training can have high classification results. Users who took part in the experiment on a regular basis, however, had better classification results. On the whole, the average recognition accuracy is enough for the subjects to navigate the robot tracking the planned trajectory only controlled by BMI.

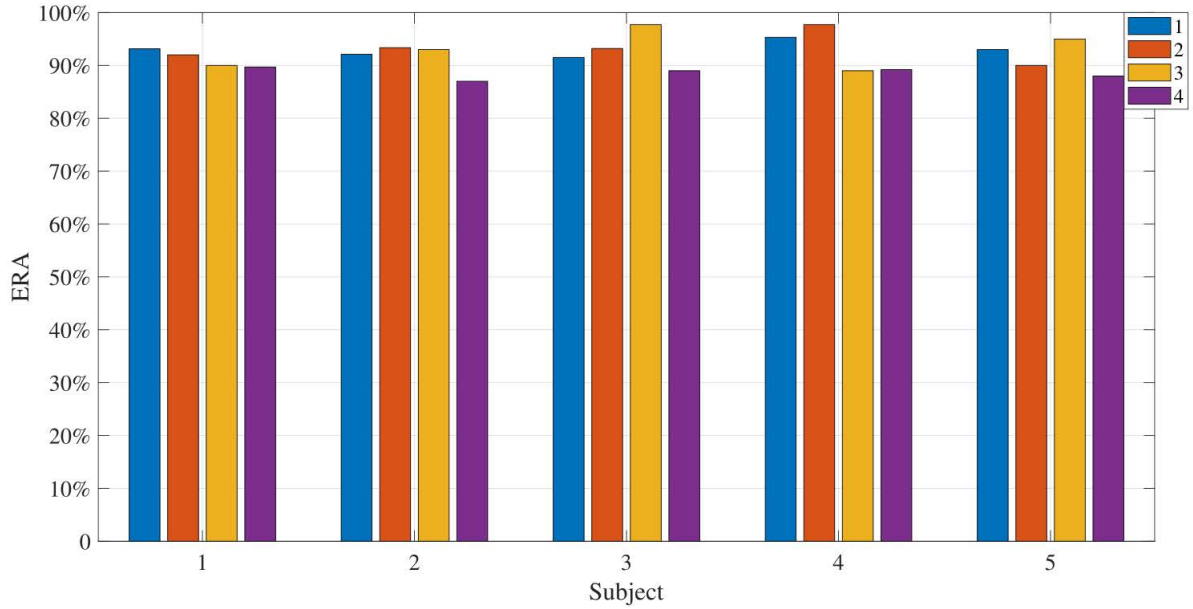

Figure 5. The ERA of the subjects.

6.3. Results and analysis of motion

By using the CCA recognition method, the four stimulus frequencies EEG signals will be decoded with labels 1–4. The stimulate module on the top screen is 15 Hz, and the EEG classification result with label 1 is converted to the motion control instruction of the robot as go forward. Similarly, stimulate module on the bottom screen, left screen and right screen are 8.57 Hz, 10 Hz, 12 Hz, and the EEG classification results are 4, 2, 3 which are converted to the other instruction of the robot as "move backward", "turn anti-clockwise", and "turn clockwise". Then, the subjects movement intentions can be decoded by using CCA classification algorithm, and the results with different labels correspond to the different motion commands of the mobile robot.

On the wall directly in front of the robot, there is a red rectangle. The task of the brain-control is to control the robot move to the the front of the red rectangle by EEG [32, 33]. In the experiment, the visual feedback will appear on the display screen and feed back to the subjects. One thing to note is that the goal position has a certain ambiguity, that is to say the goal positions are within a certain range. All trajectory and motion control calculations are based on the world coordinate system and the robot body coordinate system. So the trajectories and goal positions of all subjects are different [34,35], even the same subject in different experiments have the different trajectories and goals.

Figures 6–15 show the experiments trajectories and velocity error of all subjects. From the Figures 6, 8, 10, 12 and 14, it can be seen that the trajectories of the robot is smooth, and the planned and the followed trajectories are basically coincide. From the Figures 7, 9, 11, 13 and 15, it can be seen that the tracking error approaches to zero. This can indicate that the velocity controller involved in this paper can control the robot motion. From the trajectories and the errors of all the subject, it can be seen that all subjects can successfully completed the given task. All subjects in the experiment can use EEG to control the mobile robot along the predicted trajectory from the start point to reach the goal position.

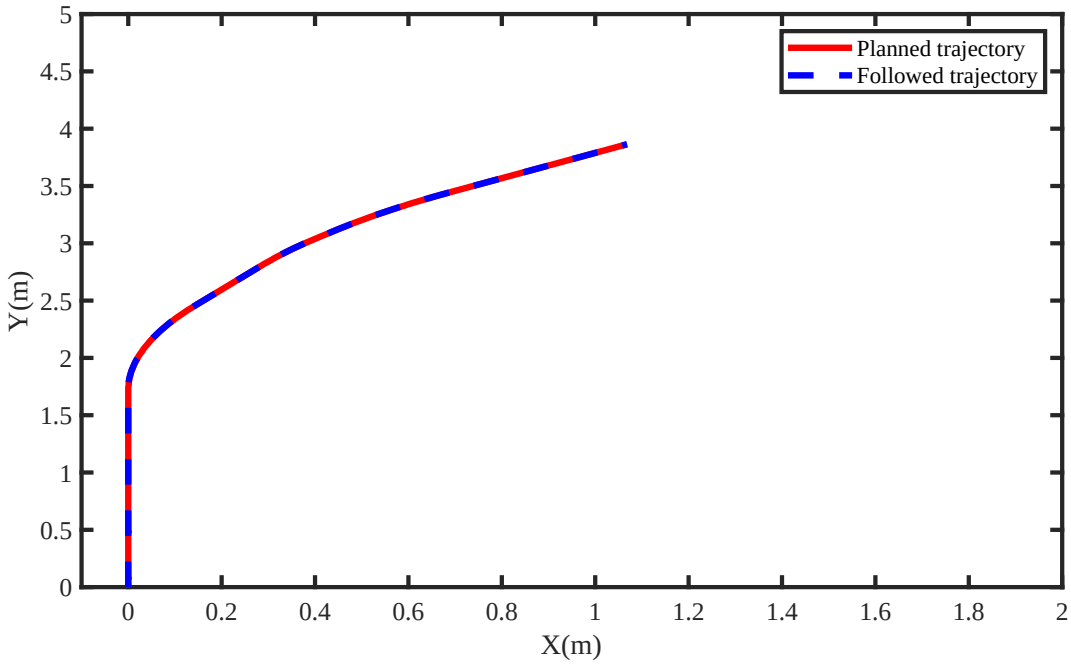

Figure 6. The trajectory of subject 1.

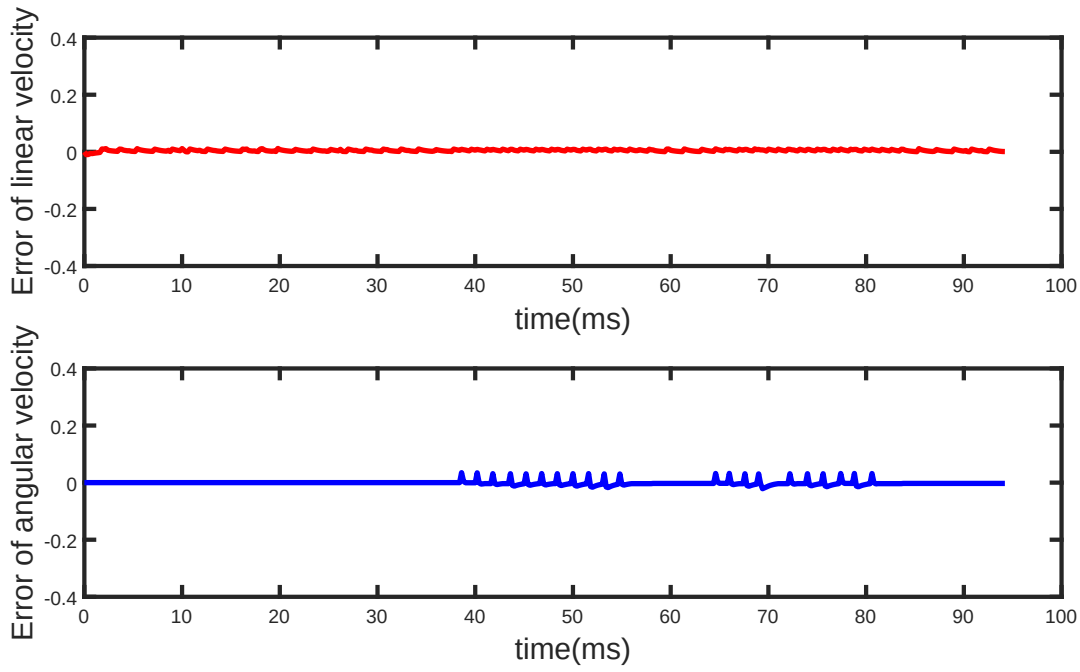

Figure 7. The linear and angular velocity error of subject 1.

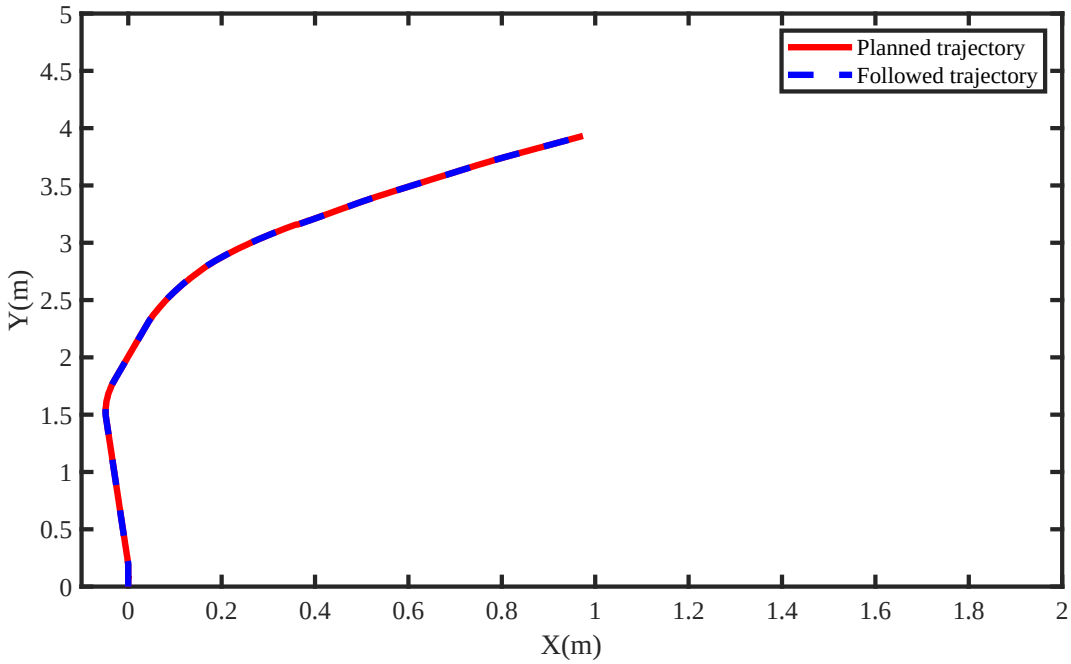

Figure 8. The trajectory of subject 2.

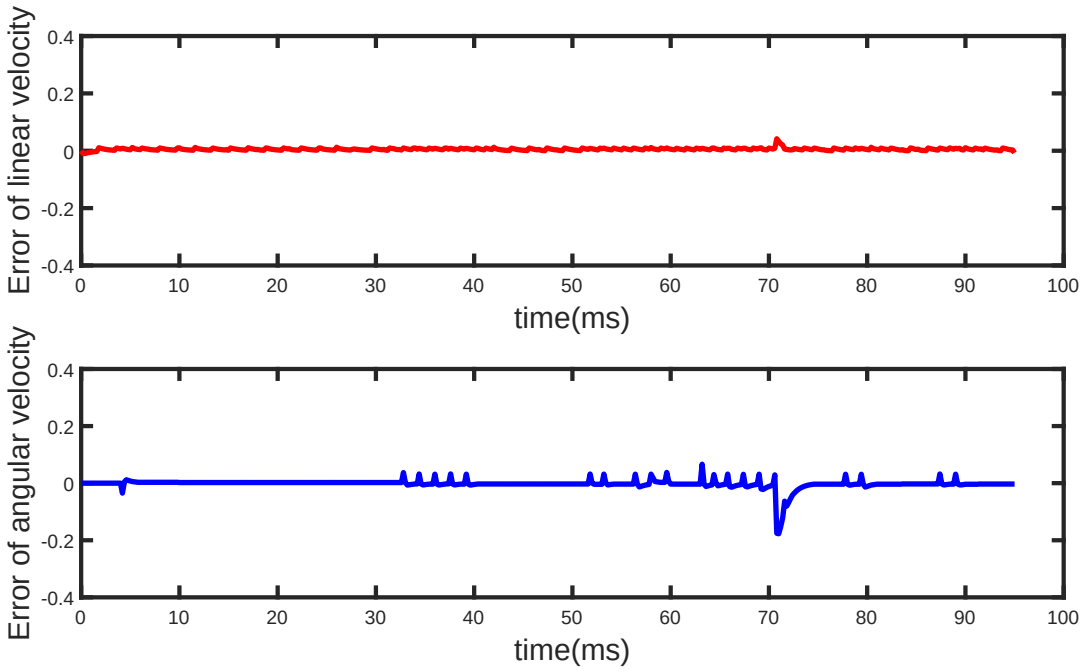

Figure 9. The linear and angular velocity error of subject 2.

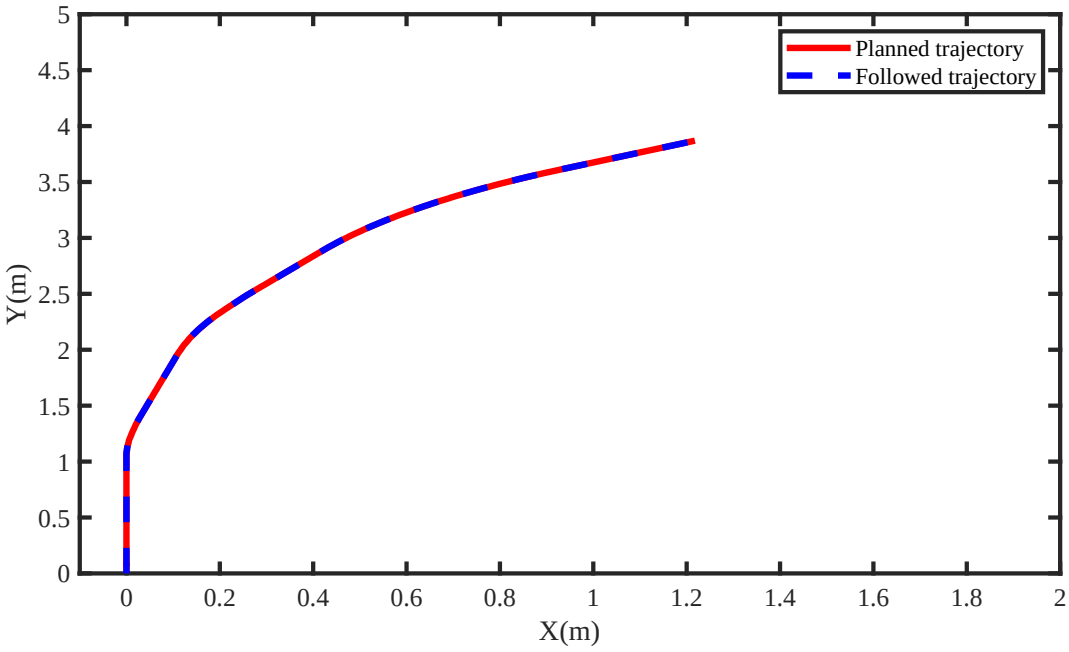

Figure 10. The trajectory of subject 3.

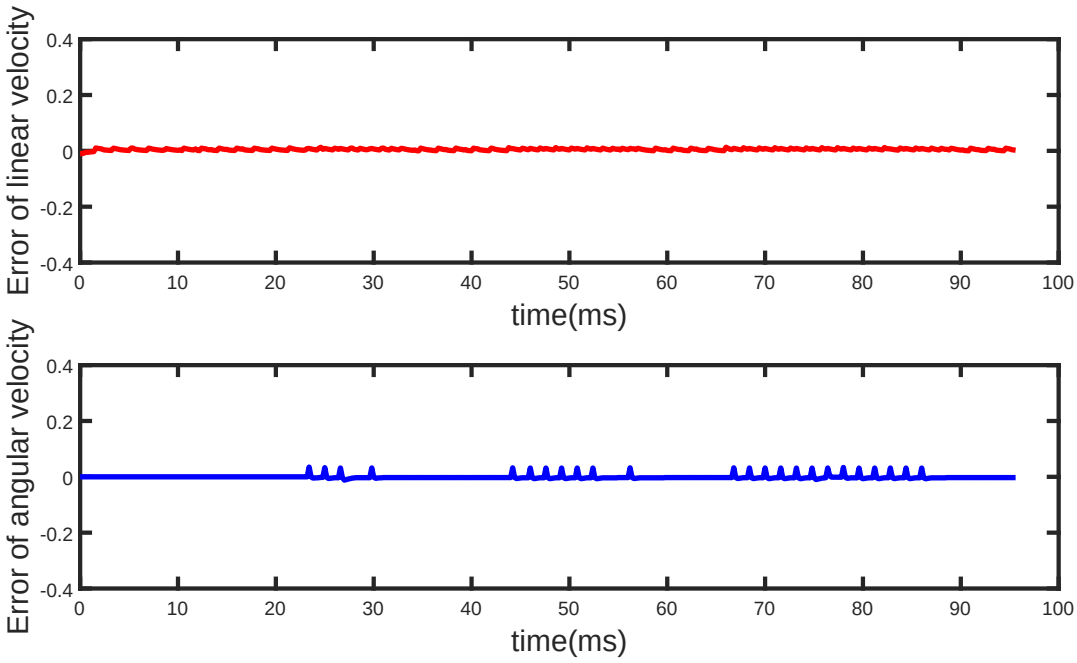

Figure 11. The linear and angular velocity error of subject 3.

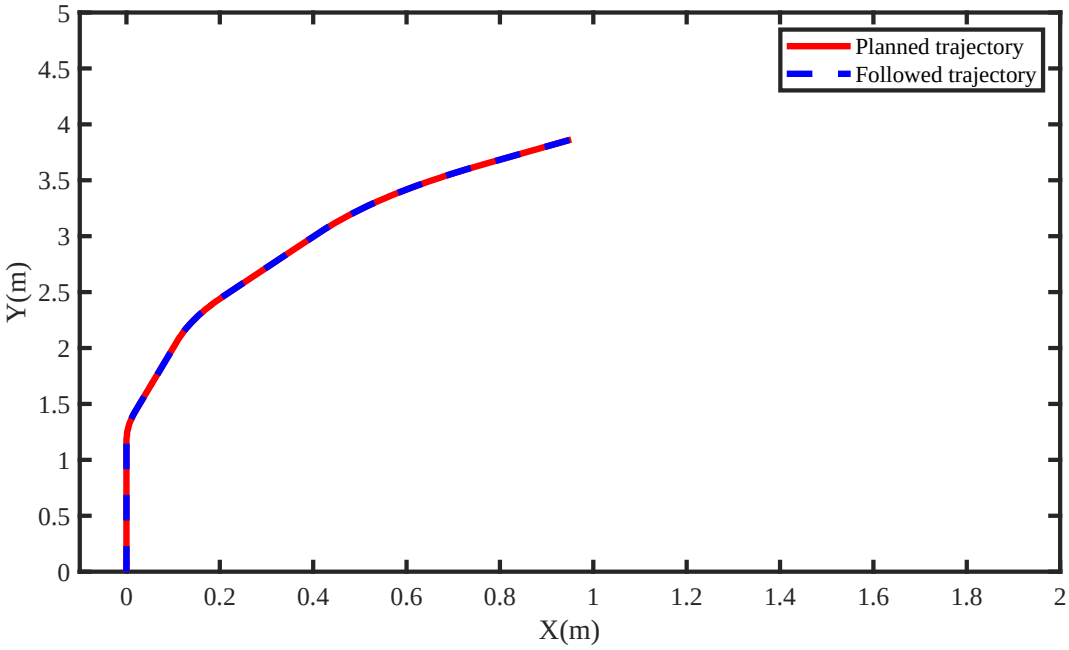

Figure 12. The trajectory of subject 4.

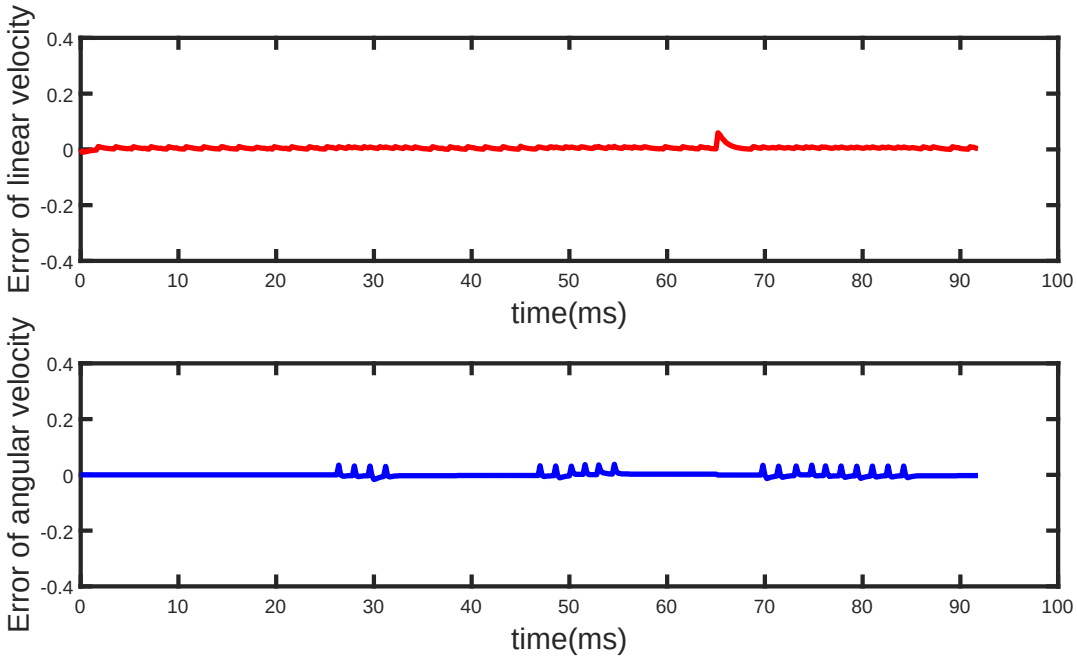

Figure 13. The linear and angular velocity error of subject 4.

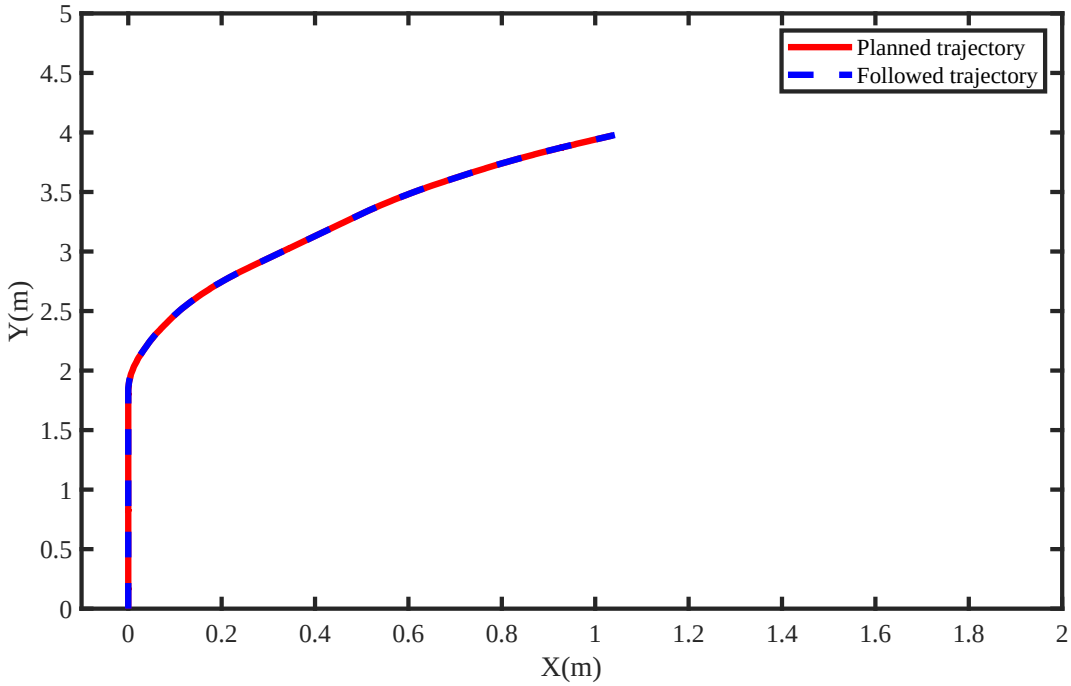

Figure 14. The trajectory of subject 5.

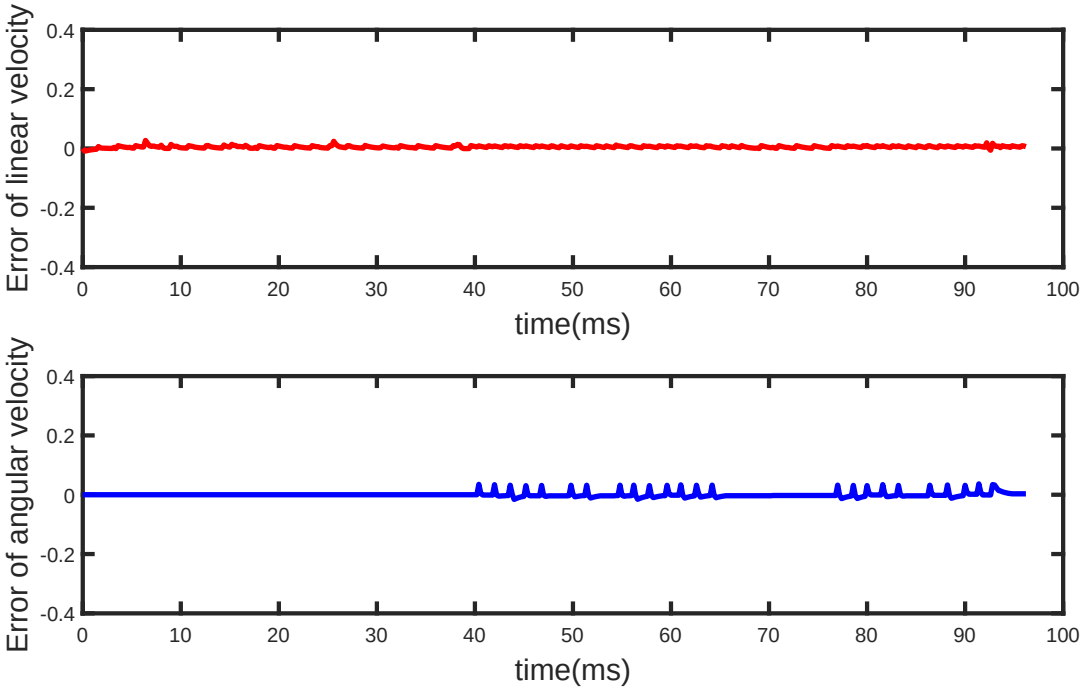

Figure 15. The linear and angular velocity error of subject 5.

7. Conclusions

The primary task is to build an EEG cooperation mobile robot motion control system that is non-intrusive. By monitoring environmental information in real time and displaying the information on the screen, EEG signals are generated through visual feedback to plan the trajectory and control the movement of the robot. The EEG recognition algorithm interprets the motion intention of the brain in real time, and the classification results are converted into the motion control commands of the mobile robot. Then, controller which can satisfy the kinematic and nonholonomic constraint of the robot will guarantee the good performance to track the planned trajectory. Finally, the experiments validate the overall feasibility and performance of the proposed system. In the future, the intelligence of mobile robot will be improved by adding sensors, we will focus on obstacle avoidance and synchronous localization and mapping of brain-controlled robot in indoor environment.

Acknowledgments

This paper is supported in part by the National Natural Science Foundation of China (Grant No. 62003312), and Science and Technology Development Project of Henan Province (212102210366), Special Plan of Basic Scientific Research Service of Henan Provincial Education Department (20KYYWF115), Innovation Incubator project of Zhengzhou University of Light Industry (DQX20190106), Key scientific research Project of colleges and universities in Henan Province (20A413011), Doctor Foundation project of Zhengzhou University of Light Industry (2018BSJJ007), Young Innovative Talents Project of Guangdong Provincial Department of Education (2018KQNCX328).

Conflict of interest

The authors declare there is no conflict of interest.

References

1. Z. Li, W. Yuan, S. Zhao, Z. Yu, Y. Kang, C. P. Chen, Brain-actuated control of dual-arm robot manipulation with relative motion, *IEEE Trans. Cognit. Dev. Syst.*, **11** (2017), 51–62. https://doi.org/10.1109/TCDS.2017.2770168
2. Y. Yuan, W. Su, Z. Li, G. Shi, Brain-computer interface-based stochastic navigation and control of a semiautonomous mobile robot in indoor environments, *IEEE Trans. Cognit. Dev. Syst.*, **11** (2018), 129–141. https://doi.org/10.1109/TCDS.2018.2885774
3. Y. Chae, J. Jeong, S. Jo, Toward brain-actuated humanoid robots: asynchronous direct control using an EEG-based BCI, *IEEE Trans. Rob.*, **28** (2012), 1131–1144. https://doi.org/10.1109/TRO.2012.2201310
4. L. Tonin, F. C. Bauer, J. D. R. Millan, The role of the control framework for continuous teleoperation of a brain-machine interface-driven mobile robot, *IEEE Trans. Rob.*, **36** (2019), 78–91. https://doi.org/10.1109/TRO.2019.2943072

5. S. Zhao, Z. Li, R. Cui, Y. Kang, F. Sun, R. Song, Brain-machine interfacing-based teleoperation of multiple coordinated mobile robots, *IEEE Trans. Ind. Electron.*, **64** (2016), 5161–5170. https://doi.org/10.1109/TIE.2016.2606089
6. X. Deng, Z. Yu, C. Lin, Z. Gu, Y. Li, A bayesian shared control approach for wheelchair robot with brain machine interface, *IEEE Trans. Neural Syst. Rehabil. Eng.*, **28** (2019), 328–338. https://doi.org/10.1109/TNSRE.2019.2958076
7. Z. Li, S. Zhao, J. Duan, C. Y. Su, C. Yang, X. Zhao, Human cooperative wheelchair with brain-machine interaction based on shared control strategy, *IEEE/ASME Trans. Mechatron.*, **22** (2016), 185–195. https://doi.org/10.1109/TMECH.2016.2606642
8. B. Rebsamen, E. Burdet, C. Guan, H. Zhang, C. Teo, Q. Zeng, et al., Controlling a wheelchair indoors using thought, *IEEE Intell. Syst.*, **22** (2007), 18–24. https://doi.org/10.1109/MIS.2007.26
9. E. Yin, Z. Zhou, J. Jiang, Y. Yu, D. Hu, A dynamically optimized SSVEP brain-computer interface (BCI) speller, *IEEE Trans. Biomed. Eng.*, **62** (2014), 1147–1456. https://doi.org/10.1109/TBME.2014.2320948
10. T. Vouga, K. Z. Zhuang, J. Olivier, M. A. Lebedev, M. A. Nicolelis, M. Bouri, et al., EXiO-A brain-controlled lower limb exoskeleton for rhesus macaques, *IEEE Trans. Neural Syst. Rehabil. Eng.*, **25** (2017), 131–141. https://doi.org/10.1109/TNSRE.2017.2659654
11. F. Janabi-Sharifi, I. Hassanzadeh, Experimental analysis of mobile-robot teleoperation via shared impedance control, *IEEE Trans. Syst. Man Cybern. Part B Cybern.*, **41** (2010), 591–606. https://doi.org/10.1109/TSMCB.2010.2073702
12. C. Escolano, J. M. Antelis, J. Minguez, A telepresence mobile robot controlled with a nonoimvasive brain-computer interface, *IEEE Trans. Syst. Man Cybern. Part B Cybern.*, **42** (2011), 793–804. https://doi.org/10.1109/TSMCB.2011.2177968
13. I. Iturrate, J. M. Antelis, A. Kubler, J. Minguez, A noninvasive brain-actuated wheelchair based on a P300 neurophysiological protocol and automated navigation, *IEEE Trans. Rob.*, **25** (2009), 614–627. https://doi.org/10.1109/TRO.2009.2020347
14. A. Kelly, N. Chan, H. Herman, D. Huber, R. Meyers, P. Rander, et al., Real-time photorealistic virtualized reality interface for remote mobile robot control, *Int. J. Rob. Res.*, **30** (2011), 384–404. https://doi.org/10.1177/0278364910383724
15. M. Lepetic, G. Klancar, I. Skrjanc, D. Matko, B. Potocnik, Time optimal path planning considering acceleration limits, *Rob. Auton. Syst.*, **45** (2003), 199–210. https://doi.org/10.1016/j.robot.2003.09.007
16. T. C. Liang, J. S. Liu, G. T. Hung, Y. Z. Chang, Practical and flexible path planning for car-like mobile robot using maximal-curvature cubic spiral, *Rob. Auton. Syst.*, **52** (2005), 312–335. https://doi.org/10.1016/j.robot.2005.05.001
17. E. Papadopoulos, I. Papadimitriou, I. Poulakakis, Polynomial-based obstacle avoidance techniques for nonholonomic mobile manipulator systems, *Rob. Auton. Syst.*, **51** (2005), 229–247. https://doi.org/10.1016/j.robot.2005.03.006
18. L. Fowler, J. Rogers, Bzier curve path planning for parafoil terminal guidance, *J. Aerosp. Inf. Syst.*, **11** (2014), 300–315. https://doi.org/10.2514/1.I010124

19. J. R. Wolpaw, N. Birbaumer, D. J. McFarland, G. Pfurtscheller, T. M. Vaughan, Brain-computer interfaces for communication and control, *Clin. Neurophysiol.*, **113** (2002), 767–791. https://doi.org/10.1016/S1388-2457(02)00057-3

20. E. Candes, J. Romberg, T. Tao, Robust uncertainty principles: Exact signal reconstruction from highly incomplete frequency information, *IEEE Trans. Inf. Theory*, **52** (2006), 489–509. https://doi.org/10.1109/TIT.2005.862083

21. J. W. Choi, R. E. Curry, G. H. Elkaim, Continuous curvature path generation based on Bzier curves for autonomous vehicles, *IAENG Int. J. Appl. Math.*, **40** (2010), 91–101. https://doi.org/10.1016/j.cej.2005.12.011

22. K. G. Jolly, R. S. Kumar, R. vijayakumar, A Bezier curve based path planning in a multi-agent robot soccer system without violating the acceleration limits, *Rob. Auton. Syst.*, **57** (2009), 23–33. https://doi.org/10.1016/j.robot.2008.03.009

23. Z. Sun, F. Li, X. Duan, L. Jin, Y. Lian, S. Liu, et al., A novel adaptive iterative learning control approach and human-in-the-loop control pattern for lower limb rehabilitation robot in disturbances environment, *Auton. Rob.*, **45** (2021), 595–610. https://doi.org/10.1007/s10514-021-09988-3

24. L. Jin, J. Li, Z. Sun, J. Lu, F. Wang, Neural dynamics for computing perturbed nonlinear equations applied to ACP-based lower limb motion intention recognition, *IEEE Trans. Syst. Man Cybern.: Syst.*, **52** (2021), 5105–5113. https://doi.org/10.1109/TSMC.2021.3114213

25. Z. Sun, G. Wang, L. Jin, C. Cheng, B. Zhang, J. Yu, Noise-suppressing zeroing neural network for online solving time-varying matrix square roots problems: A control-theoretic approach, *Expert Syst. Appl.*, **192** (2022), 116272. https://doi.org/10.1016/j.eswa.2021.116272

26. Z. Sun, T. Shi, L. Jin, B. Zhang, Z. Pang, J. Yu, Discrete-time zeroing neural network of $O(\tau_4)$ pattern for online solving time-varying nonlinear optimization problem: Application to manipulator motion generation, *J. Franklin Inst.*, **358** (2021), 7203–7220. https://doi.org/10.1016/j.jfranklin.2021.07.006

27. W. Qi, H. Su, A cybertwin based multimodal network for ecg patterns monitoring using deep learning, *IEEE Trans. Ind. Inf.*, **18** (2022), 6663–6670. https://doi.org/10.1109/TII.2022.3159583

28. K. Liu, Y. Liu, Y. Zhang, L. Wei, Z. Sun, L. Jin, Five-step discrete-time noise-tolerant zeroing neural network model for time-varying matrix inversion with application to manipulator motion generation, *Eng. Appl. Artif. Intell.*, **103** (2021), 104306. https://doi.org/10.1016/j.engappai.2021.104306

29. H. Su, Y. Hu, H. R. Karimi, A. Knoll, G. Ferrigno, E. D. Momi, Improved recurrent neural network-based manipulator control with remote center of motion constraints: Experimental results, *Neural Networks*, **131** (2020), 291–299. https://doi.org/10.1016/j.neunet.2020.07.033

30. H. Su, W. Qi, Y. Schmirander, S. E. Ovur, S. Cai, X. Xiong, A human activity-aware shared control solution for medical human–robot interaction, *Assem. Autom.*, **42** (2022), 388–394. https://doi.org/10.1108/AA-12-2021-0174

31. H. Su, A. Marian, S. E. Ovur, A. Menciassi, G. Ferrigno, E. D. Momi, Toward teaching by demonstration for robot-assisted minimally invasive surgery, *IEEE Trans. Autom. Sci. Eng.*, **18** (2021), 484–494. https://doi.org/10.1109/TASE.2020.3045655

32. J. Chen, H. Qiao, Motor-cortex-like recurrent neural network and multitask learning for the control of musculoskeletal systems, *IEEE Trans. Cognit. Dev. Syst.*, **14** (2020), 424–436. https://doi.org/10.1109/TCDS.2020.3045574

33. H. Su, S. E. Ovur, X. Zhou, W. Qi, G. Ferrigno, E. D. Momi, Depth vision guided hand gesture recognition using electromyographic signals, *Adv. Rob.*, **34** (2020), 985–997. https://doi.org/10.1080/01691864.2020.1713886

34. H. Su, W. Qi, C. Yang, J. Sandoval, G. Ferrigno, E. De Momi, Deep neural network approach in robot tool dynamics identification for bilateral teleoperation, *IEEE Rob. Autom. Lett.*, **5** (2020), 2943–2949. https://doi.org/10.1109/LRA.2020.2974445

35. J. Chen, H. Qiao, Muscle-synergies-based neuromuscular control for motion learning and generalization of a musculoskeletal system, *IEEE Trans. Syst. Man Cybern.: Syst.*, **51** (2020), 3993–4006. https://doi.org/10.1109/TSMC.2020.2966818

AIMS Press